Morphological transitions in the development of a cylindrical crystal

2003 J. Phys.: Condens. Matter 15 1137

(http://iopscience.iop.org/0953-8984/15/7/310)

INSTITUTE OF PHYSICS PUBLISHING JOURNAL OF PHYSICS: CONDENSED MATTER

J. Phys.: Condens. Matter **15** (2003) 1137–1146 PII: S0953-8984(03)57895-X

Morphological transitions in the development of a cylindrical crystal

L M Martjushev and E M Sal'nikova

Institute of Industrial Ecology, Ural Division, Russian Academy of Sciences, Yekaterinburg 620219, Russia

E-mail: mlm@ecko.uran.ru

Received 7 January 2003
Published 10 February 2003
Online at stacks.iop.org/JPhysCM/15/1137

Abstract

We consider non-equilibrium growth of a cylindrical crystal from solution, taking account of the arbitrary rate of kinetic processes at the boundary and the linear dependence of the growth rate on the supersaturation. We calculate full morphological diagrams, using linear analysis for the stability and the principle of maximum entropy production. The possibility of coexistence of several morphological phases is revealed. We demonstrate that the mass of the crystal increases abruptly in the morphological transition.

1. Introduction

Problems of structuring in non-equilibrium crystallization (e.g., development of dendrites) have long remained topical in materials science and physical metallurgy [1, 2]. However, in recent decades such examples of self-organization have also attracted the attention of theorists [3, 4] in connection with the intensive development of the physics of open non-equilibrium systems.

Here, one of the existing problems is as follows. Methods for analytically calculating the boundaries of metastable and labile regions have not been developed to their full extent as yet, although regions of parameters controlling the non-equilibrium crystallization, in which different morphologies may coexist, have been found in numerous experimental studies [5–7].

To calculate the full morphological diagram (with stable, metastable, and absolutely unstable regions), it has been proposed [8, 9] that one could use the principle of maximum entropy production [10] in combination with linear analysis for the morphological stability. Henceforth, we mean by 'the principle of maximum entropy production' the following: if there are perturbations of sufficient amplitude in a system, the existing state is that with the maximum entropy production. At first sight, this principle contradicts the well-known Prigogine principle of minimum entropy production [11]. However, as shown in the literature (see, e.g., [10, 12]), the validity regions of the principles of maximum and minimum entropy production are completely different. Prigogine's principle states that, in a stationary slightly non-equilibrium state, the system will be characterized by the minimum entropy production [11]; i.e., the

behaviour of the system near a single stationary state is considered. The principle of maximum entropy production shows how a non-equilibrium system evolves in the presence of several possible stationary states, with a spontaneous non-equilibrium system considered. Correspondingly, these principles refer to different types of variational problem (in Prigogine's formulation, thermodynamic fluxes are invariable at the boundary). However, as shown in [10], Prigogine's principle is a consequence of the principle of maximum entropy production for linear processes. Previously, this principle of maximum entropy production has been applied to problems of crystallization from solution/melt in order to analyse experimental data [13–16].

In [8, 9], the problem of morphological selection was for the first time considered analytically using this principle in a consistent way. The basic concept of these studies is that the application of the principle of maximum entropy production yields the binodal of the non-equilibrium morphological transition (the point of instability with respect to finite small perturbations), rather than the spinodal (the point of instability with respect to infinitesimal perturbations).

In [8, 9], only the case of morphological stability in the growth of a crystal (spherical and cylindrical) was considered under the assumption of infinitely fast isotropic kinetic processes on the surface, i.e., with the crystallization rate limited solely by diffusion. A later study [17] extended the method to a more general case: growth of an originally spherical nucleus at an arbitrary rate of surface processes. The calculations that we carry out in this study not only make it possible to describe a vast body of experimental data on the crystallization of quasi-isotropic systems, but also show that the rate of the surface processes strongly affects the possible number of simultaneously coexisting different morphological phases. However, to gain full insight into how the rate of surface processes affects morphological transitions, we should consider a similar problem for another initial geometry of the nucleus. Apparently, with the exception of the spherical case, solely the problem with a nucleus of cylindrical symmetry can be considered analytically from the beginning to the end. At the same time, this problem is important practically, since its solution is frequently used to understand the conditions for appearance of secondary branches in the primary branch in dendrite formation [18].

Thus, the aim of the present study is to apply the approach proposed in [8, 9] to analysis of the problem of morphological selection in non-equilibrium growth of a cylindrical crystal, with account taken of the finite rate of kinetic processes at the boundary and the linear dependence of the growth rate on the supersaturation.

2. Linear analysis for the morphological stability

A linear analysis for the stability in growth of a cylindrical particle from a melt was carried out in [19]. However, the specificity of boundary conditions for the case of crystallization from solution and the incompleteness of the results presented in [19] necessitate an independent linear analysis for the morphological stability. In the case of growth of a slightly distorted cylindrical particle from solution, the problem can be stated as follows:

(1) Crystallization occurs in isothermal–isobaric conditions. The free surface energy and the kinetic coefficient are considered to be isotropic.
(2) The concentration field is described by the diffusion equation $\partial c/\partial t = D\,\nabla^2 c$.
(3) It is assumed that an arbitrary small distortion of the cylinder can be regarded as a superposition of harmonic functions of the type $F(\varphi, z) = \cos(k\varphi)\cos(k_z z/R)$ where z and φ are cylindrical coordinates, k is a positive integer, k_z can take any real value, and R is the radius of the unperturbed cylinder. The behaviour under perturbation with a single harmonic is considered.

(4) The concentration in solution satisfies the following boundary conditions:

$$c(\infty, t) = C_\infty, \qquad c(r, t) = C_{\text{int}}, \tag{1}$$

$$V = \dot{R} + \dot{\delta} F(\varphi, z) = \frac{D}{C} \frac{\partial c}{\partial r}\bigg|_r = \frac{\beta}{C}(C_{\text{int}} - C_{\text{int eq}}), \tag{2}$$

where V is the local growth rate, $\dot{R} \equiv \mathrm{d}R/\mathrm{d}t$, $\dot{\delta} \equiv \mathrm{d}\delta/\mathrm{d}t$, t is time, c is the current concentration of the solution, $r = R(t) + \delta(t)F(\varphi, z)$ is the shape of the distorted cylinder surface, $\delta(t)$ is the perturbation amplitude ($\delta \ll R$), D is the diffusion coefficient, β is the kinetic crystallization coefficient, C is the crystal density, C_∞ is the solution concentration far away from the crystal, C_{int} is the concentration near the surface of arbitrary type, and $C_{\text{int eq}} = C_{\text{int}}(\beta \to \infty)$ is the equilibrium concentration of the dissolved substance near the surface of arbitrary type.

We write the boundary condition (2) on the assumption that the concentration of the dissolved substance is negligibly small as compared with the crystal density. This assumption, much simplifying the solution of the problem, has good validity for many real systems crystallizing from solution.

We restrict the consideration to the case $(C_\infty - C_{\text{int}})/(C - C_{\text{int}}) \ll 1$ (which, is, in fact, satisfied for most of the solutions [20, 21]). In this approach, in accordance with [19, 21], the solution to the diffusion equation with boundary conditions (1) and (2) coincides with high precision with that to the Laplace equation ($\nabla^2 c = 0$) with boundary conditions $c(R_\lambda) = C_\infty$, $c(r) = C_{\text{int}}$, and (2). Here, $R_\lambda = R/\nu\lambda$ and $\ln \nu^2 = 0.5772$ is the Euler constant, with λ found from the equation $\lambda^2 \ln(\nu^2\lambda^2) + (C_\infty - C_{\text{int}})/(C - C_{\text{int}}) = 0$. Then, in the linear approximation, the solution to our problem has the following form:

$$c(r, \varphi, z) = C_\infty + \frac{C_\infty - C_{R\,\text{eq}}}{A_\lambda + \alpha\rho} \ln \frac{r}{R_\lambda} + \left(\frac{C_0\Gamma}{R^2} K - \frac{(1 + \alpha\rho)}{R} \frac{C_\infty - C_{R\,\text{eq}}}{A_\lambda + \alpha\rho} \right) \times \frac{\delta \Re_k(k_z r/R) F(\varphi, z)}{\Re_k(k_z)(1 + \alpha\rho H)}, \tag{3}$$

$$\dot{R} = \frac{D}{C} \frac{C_\infty - C_{R\,\text{eq}}}{R(A_\lambda + \alpha\rho)}, \tag{4}$$

$$\dot{\delta}(t) = \frac{-D\delta}{CR^2} \left[\frac{C_\infty - C_{R\,\text{eq}}}{A_\lambda + \alpha\rho} + \left(\frac{C_0\Gamma}{R} K - (1 + \alpha\rho) \frac{C_\infty - C_{R\,\text{eq}}}{A_\lambda + \alpha\rho} \right) \frac{H}{1 + \alpha\rho H} \right], \tag{5}$$

where $A_\lambda = \ln(R_\lambda/R)$, $\alpha = D/\beta R^*$, $R^* = C_0\Gamma/(C_\infty - C_0)$ is the radius of a critical nucleus, $\rho = R^*/R$, $C_{R\,\text{eq}} = C_0(1 + \Gamma/R)$ is the equilibrium concentration of dissolved substance near an unperturbed cylindrical surface, C_0 is the equilibrium concentration of dissolved substance near a flat boundary, Γ is the surface tension coefficient, $H = H(k, k_z) = -k_z \Re'_k(k_z)/\Re_k(k_z)$, $\Re_k(k_z)$ are modified Hankel functions, $\Re'_k(k_z)$ is the derivative of a modified Hankel function [19, 21], and $K = K(k, k_z) = k^2 + k_z^2 - 1$.

It follows from expression (5) that the perturbation will grow if the crystal radius exceeds the critical radius R^{s}:

$$R^{\text{s}} = \frac{R^*}{2} \left[1 + \frac{A_\lambda K H}{H - 1} + \sqrt{\left(1 + \frac{A_\lambda K H}{H - 1} \right)^2 + 4\alpha K \frac{H}{H - 1}} \right]. \tag{6}$$

In deriving expression (6), we disregard the dependence of A_λ on R, since numerical calculations have shown that the parameter λ obtained in the $(C_\infty - C_{\text{int}})/(C - C_{\text{int}}) \approx (C_\infty - C_0)/(C - C_0)$ approximation yields an error A_λ not exceeding 2–4%.

Expressions (5) and (6) completely determine the stability of a cylindrical particle growing from solution against an infinitesimal perturbation, and, in the limit of an indefinitely large kinetic coefficient, the solution that we obtain reduces to the results of [21]. According to [8, 9], expression (6) is the equation of the spinodal of a morphological transition from stable (cylindrical) to unstable ('dendritic') growth.

3. Thermodynamic analysis for morphological stability

Let us apply the thermodynamic approach, described in detail in [9], to this problem. We find the difference in entropy production ($\Delta\Sigma$) between the cases of growth of perturbed and unperturbed cylindrical crystals. We calculate the local entropy production per unit time σ for a volume near the crystal surface, which has unit thickness and area cut out by angle $\mathrm{d}\varphi$ and length element $\mathrm{d}z$. We restrict the consideration to the dilute solution approximation, i.e., that accurate to within a constant $\sigma \sim D(\nabla c)^2/c$ [22]. In this case, we can write $\Delta\Sigma$, using (2), as

$$\Delta\Sigma \sim \left(\frac{V^2 r}{C_{\mathrm{int}}} - \frac{\dot{R}^2 R}{C_R}\right)\frac{C^2}{D}\,\mathrm{d}\varphi\,\mathrm{d}z \tag{7}$$

where C_R is the non-equilibrium concentration of the solute near the unperturbed cylindrical surface.

As shown by a numerical calculation carried out using the MathCAD software package, $\Delta\Sigma$ grows (at $F(\varphi, z) > 0$) on the interval of possible variation of the cylinder radius $[R^*, R^{\mathrm{s}}]$ and becomes zero at $R = R^{\mathrm{b}}$. According to [8, 9], the point R^{b} obtained by solving the equation

$$\Delta\Sigma = 0, \tag{8}$$

with the use of expressions (2), (4), and (5), is the binodal of the morphological transition under study.

Figure 1 shows a numerical solution R^{b} of equation (8) as a function of the parameter α. It is clear that the binodal radius decreases with increasing α, with the most significant change observed at α in the range from 10 to 100.

An essential difference of the problem with an arbitrary rate of surface processes which we consider here from that discussed previously in [8, 9] is that, in the general case, there is no local equilibrium at the crystal–solution interface. Therefore, an expression of the type $\sigma \sim D(\nabla c)^2/c$ is inapplicable to calculation of the entropy production directly on the surface. Thus, according to [22], the following expression is necessary for calculating the entropy production at the phase boundary:

$$\Delta\Sigma^{\mathrm{int}} \sim j(\mu_{\mathrm{int}} - \mu_{\mathrm{eq}})r\,\mathrm{d}\varphi\,\mathrm{d}z, \tag{9}$$

where μ_{int}, μ_{eq} are the chemical potentials of the solute with concentrations C_{int} and $C_{\mathrm{int\,eq}}$, respectively; j is the flux of the solute towards the surface.

Since, in the case of dilute solutions, the chemical potential is proportional to within an additive constant to the logarithm of the concentration ($\mu_{\mathrm{int}} \sim \ln C_{\mathrm{int}}$) and the flux $j \sim CV$ (we assume that $C \gg c$), the difference in entropy production at the surface between the perturbed and unperturbed growing cylinders is as follows:

$$\Delta\Sigma^{\mathrm{int}} \sim C\left(Vr\ln\frac{C_{\mathrm{int}}}{C_{\mathrm{int\,eq}}} - \dot{R}R\ln\frac{C_R}{C_{R\,\mathrm{eq}}}\right)\mathrm{d}\varphi\,\mathrm{d}z. \tag{10}$$

In the linear approximation, we can transform the last expression, taking account of (2), (4), and (5), to

$$\Delta\Sigma^{\mathrm{int}} \sim C\left((\dot{\delta}R + \dot{R}\delta)\ln\frac{C_R}{C_{R\,\mathrm{eq}}} + \frac{C_{\mathrm{int}} - C_R}{C_R}\dot{R}R - \frac{C_0\Gamma}{C_{R\,\mathrm{eq}}R}K\dot{R}\delta\right)\mathrm{d}\varphi\,\mathrm{d}z. \tag{11}$$

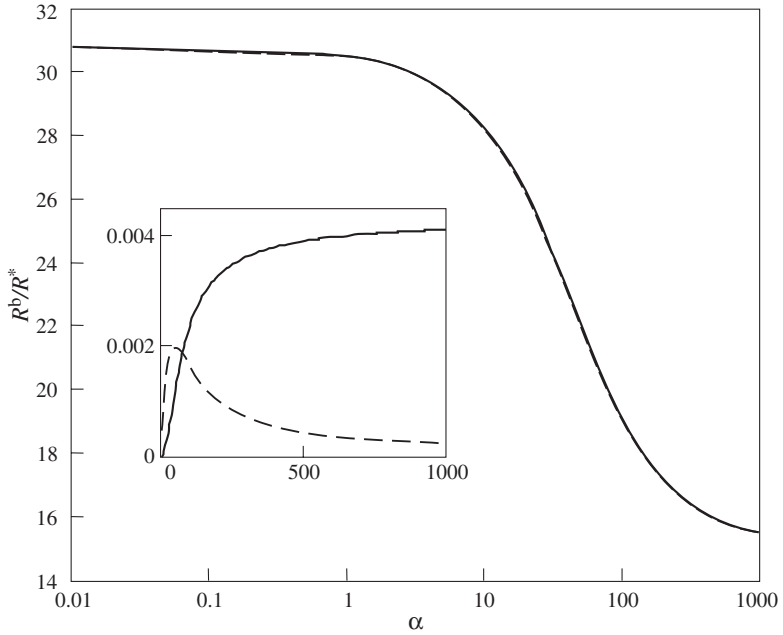

Figure 1. R^b in R^*-units versus α. The curves representing the numerical solutions to equations (8) and (12) and the analytical solution (14) coincide. In the inset, the full curve shows the relative difference of the binodal radii obtained by solving equations (8) and (12) numerically; the broken curve is the relative difference of the numerical solution to equation (8) and binodal radii obtained from analytical expression (14). The curves are plotted for $\Delta = 0.05$, $k = 2$, $k_z = 2$.

By analogy with the case considered above, we can find a point at which

$$\Delta\Sigma^{\text{int}} = 0. \tag{12}$$

The dependence of the binodal radius found from (12) on α is shown in figure 1. It can be seen that the radii obtained using (8) and (12) are indistinguishable on the given scale. However, it does not follow from the general concepts of non-equilibrium thermodynamics that the binodal radii obtained from expressions (8) and (12) must coincide. Indeed, as shown by numerical calculations, at relative supersaturations $\Delta = (C_\infty - C_0)/C_0$ exceeding 0.1, their values start to differ significantly (e.g., the difference is 25% at $\Delta = 2$ and $\alpha = 1000$). However, at $\Delta < 0.1$, the solutions to equations (8) and (12) coincide with good precision. As seen in the inset, the difference of numerical solutions to equations (8) and (12) grows with increasing α, to become 0.41% for $\alpha = 1000$ and $\Delta = 0.05$. Thus, when there is no local equilibrium at the surface and supersaturations are high, we should use, on the basis of the local principle of the maximum entropy production, expression (12) to find the binodal. However, as follows from the above calculations, the binodals obtained by the two methods coincide for a rather large range of supersaturations usually observed in experiment. At the same time, we can derive from expression (8) a simple analytical approximation for R^b, which is valid over the entire range of α-variation and describes the numerical solution with good precision. No approximation of this kind can be found from equation (12). Therefore, we consider in what follows only the approximations derived from equation (8).

Let $\Delta \ll 1$, then expression (7) transforms into

$$\Delta\Sigma \sim (\dot{R}\delta + 2\dot{\delta}R)\,\mathrm{d}\varphi\,\mathrm{d}z \sim \left(-2\rho K H + \frac{1-\rho}{A_\lambda + \alpha\rho}(H(2+\alpha\rho) - 1)\right)\delta. \tag{13}$$

Studying the behaviour of $\Delta\Sigma$ on the interval of possible variation of the crystal size, we can obtain, by analogy with the preceding calculations, an explicit expression for the binodal radius:

$$R^{\mathrm{b}} = \frac{R^*}{2}\left(1 - \frac{\alpha H}{2H-1} + \frac{2A_\lambda K H}{2H-1} + \sqrt{\left(1 - \frac{\alpha H}{2H-1} + \frac{2A_\lambda K H}{2H-1}\right)^2 + 4\alpha(2K+1)\frac{H}{2H-1}}\right). \tag{14}$$

The inset in figure 1 shows the relative error in calculating the binodal radius using the approximate formula as a function of α. The maximum error of the binodal radius calculated using formula (14) (0.2%) is obtained at $\alpha = 50$. This approximation makes it possible to describe the exact numerical solution (8) at small supersaturations with accuracy ranging from 0.05% at $\alpha = 0.1$ to 0.16% at $\alpha = 100$.

In the approximation of an infinitely fast surface kinetics ($\beta \to \infty$), equation (14) takes the form obtained previously in [9]:

$$R^{\mathrm{b\,diff}} = R^*\left(1 + \frac{2A_\lambda K H}{2H-1}\right). \tag{15}$$

In the kinetic growth mode ($\beta \to 0$), the binodal radius tends to the asymptotic value

$$R^{\mathrm{b\,kin}} = R^*(2K+1). \tag{16}$$

4. Morphological diagrams for a cylindrical crystal growing in the non-equilibrium mode

The solutions obtained for the spinodal (6) and binodal (14) radii have been used to construct morphological diagrams. In this study, we present results on the growth of a cylindrical nucleus in the presence of perturbations with respect to both φ and z. Perturbations solely in angle φ ($k_z = 0$) were analysed in [23]. Figure 2 shows morphological diagrams for regions of stable and unstable crystal growth in the intermediate and kinetic growth modes: spinodal and binodal radii are shown as functions of k_z. It can be seen that the binodals and spinodals belonging to different harmonics may intersect. Figure 2(a) illustrates the coexistence of three phases (metastable cylindrical and two phases with developing perturbations belonging to harmonics $k = 1$ and 2) at $k_z > 5.5$ and $\alpha = 1$ (the intermediate-growth mode). We now consider this case in more detail. Let the system, for the sake of definiteness, be characterized by a perturbation in z, e.g., $k_z = 6.5$, and arbitrary perturbations in φ. Then, the cylindrical crystal grows along the AC line. This growth is stable as far as point A. If the cylinder radius lies within the interval AB, the growth becomes metastable with respect to the perturbation $k = 1$. On this interval, loss of stability is only possible in the presence of a perturbation with small, but not infinitesimal amplitude, and the crystal may both continue its cylindrical growth and lose stability against perturbations $k = 1$, $k_z = 6.5$. The fraction of stable cylindrical crystals decreases with increasing radius. Beginning at point B, the crystal size reaches the radius of the binodal with respect to the perturbation $k = 2$, $k_z = 6.5$. Consequently, both stable cylindrical growth and unstable growth with development of perturbations $k = 1$ and/or $k = 2$ are possible on the BC interval. Beginning at point C (the size of the spinodal for the perturbation $k = 1$, $k_z = 6.5$), all the remaining cylindrical crystals lose stability against an infinitesimal perturbation $k = 1$. As mentioned in [9], metastable regions also intersect in the diffusion growth mode at cylindrical geometry. In the kinetic growth mode represented

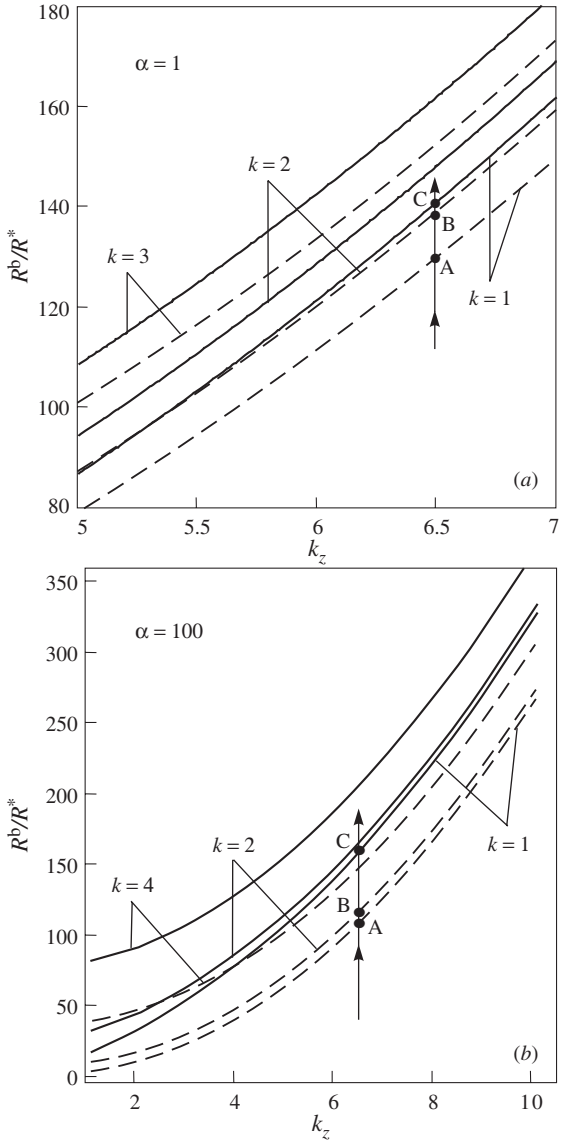

Figure 2. Radii of the spinodal R^s (full curves) and binodal R^b (broken curves) of the morphological transition as a functions of k_z in (a) the intermediate and (b) the kinetic-growth mode. Stable growth is observed below the binodal, and absolutely unstable growth above the binodal; the metastable region lies in between. The curves are plotted for $\Delta = 0.05$.

in figure 2(b), the number of coexisting phases increases to 5 at $k_z = 6.5$ and $\alpha = 100$. Comparison of figures 2(a) and (b) shows that the number of coexisting morphological phases grows with increasing α. For example, at $\Delta = 0.05$ and $k_z = 8$, 6, and 10, morphological phases can coexist at $\alpha = 150$ and 1000. Thus, in any growth mode of a cylindrical crystal, overlapping of metastable regions belonging to different perturbing harmonics is possible, which leads to coexistence of a large number of morphological phases.

Let us now consider how the mass of a crystal changes in the morphological transition described. By analogy with the entropy production, we calculate the difference between

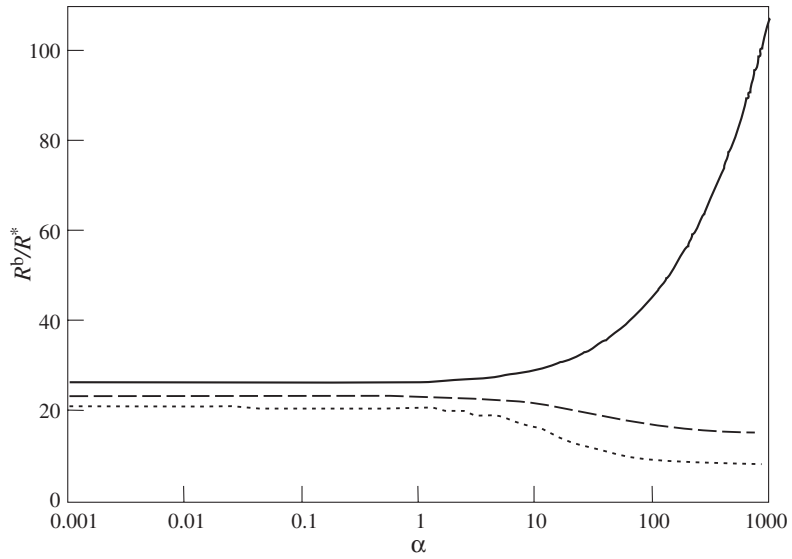

Figure 3. Radii R^s (full curve), R^b (broken curve), and R^I (dotted curve) versus parameter α for $k = 2, k_z = 2$ at relative supersaturation $\Delta = 0.05$.

the gain in crystal mass per unit time in the growth of perturbed $(dN/dt)_p$ and unperturbed $(dN/dt)_n$ cylindrical crystals for a solution volume $r\,d\varphi\,dz$ of unit thickness near the crystal surface:

$$\left(\frac{dN}{dt}\right)_p - \left(\frac{dN}{dt}\right)_n = C(Vr - \dot{R}R)\,d\varphi\,dz \sim \frac{D(C_\infty - C_0)\rho}{R^*} \times \left(\frac{(\alpha\rho + 1)(1 - \rho)}{\alpha\rho + A_\lambda} - \rho K\right)\frac{H}{1 + \alpha\rho H}. \tag{17}$$

Analysis of (17) shows that, beginning with a certain crystal size R^I, the flux of the crystallizing substance arriving from solution to the perturbed surface starts to exceed that towards the unperturbed surface (18):

$$R^I = 0.5R^*\left[1 + A_\lambda K - \alpha + \sqrt{(1 + A_\lambda K - \alpha)^2 + 4\alpha(K + 1)}\right]. \tag{18}$$

Figure 3 shows dependences of the radii R^s, R^b, and R^I on α. It can be seen that the radius of absolute instability decreases with increasing kinetic coefficient, whereas the binodal radius, by contrast, increases, which results in the width of the metastable region $[R^b, R^s]$ decreasing. The metastable zone also becomes smaller with increasing numbers of perturbing harmonics.

It can be seen from figure 3 that R^I is always smaller than R^b in any growth mode. As a result, the mass of a crystal always increases abruptly in the morphological transition (figure 4). The discontinuous change in the case of a morphological transition from stable growth to unstable growth with respect to small finite perturbations occurs on the interval $[R^b, R^s]$. If we assume that the transition occurs at the binodal point, the jump amplitude can be found by substituting the binodal radius (14) into expression (17). Numerical analysis of expression (17) shows that the discontinuous change in the rate of mass gain falls with decreasing kinetic coefficient of crystallization (figure 4(*a*)) and relative supersaturation (figure 4(*b*)), and also with growing surface tension coefficient (figure 4(*c*)) and numbers of perturbing harmonics.

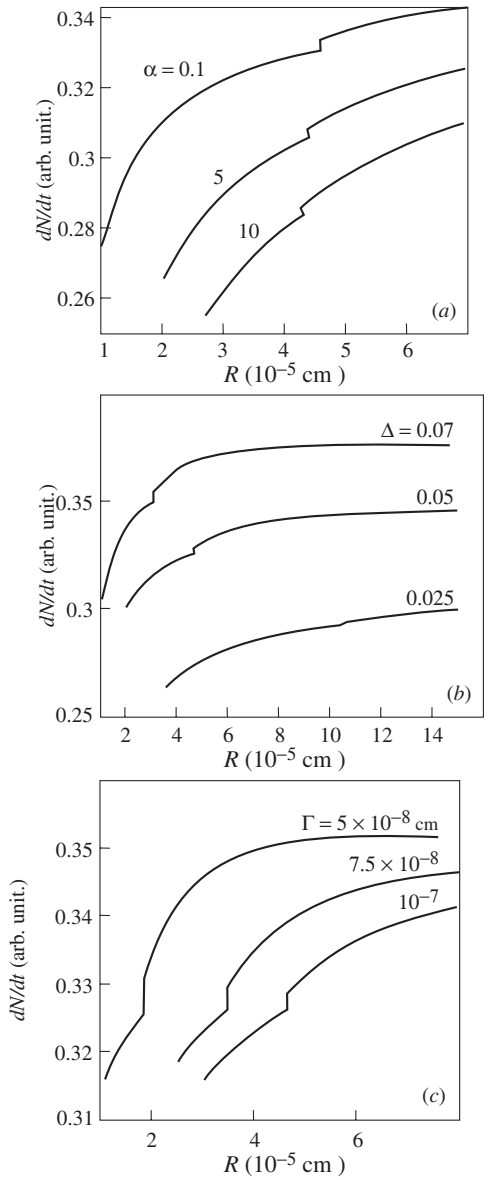

Figure 4. Rate of mass gain, dN/dt, versus crystal size R in the morphological transition at the binodal point for $k = 2, k_z = 2$. (*a*) $\Delta = 0.05, \Gamma = 10^{-7}$ cm; (*b*) $\alpha = 1, \Gamma = 10^{-7}$ cm; (*c*) $\alpha = 1$, $\Delta = 0.05$.

Such a behaviour is in qualitative agreement with the results obtained previously for the spherical geometry [17].

5. Conclusions

Thus, we have performed, for the first time, an analytical study of morphological transitions in a growing cylindrical crystal in an arbitrary growth mode, using the approach proposed

previously in [8, 9]. We have revealed regions of control parameters in which different morphological phases can coexist. Calculations have shown that our conclusions are for the most part in qualitatively agreement with the results obtained for spherical geometry [17]. However, in contrast to the spherical case, coexistence of different morphological phases can be observed in both the kinetic and the diffusion growth modes for a cylindrical crystal.

References

[1] Chalmers B 1964 *Principles of Solidification* (New York: Wiley)
[2] Kurz W and Fisher D J 1992 *Fundamentals of Solidification* (Zurich: Trans Tech)
[3] Langer J S 1980 *Rev. Mod. Phys.* **52** 1–28
[4] Cross M C and Hohenberg P C 1993 *Rev. Mod. Phys.* **65** 851–1112
[5] Sawada Y, Perrin B, Tabeling P and Bouissou P 1991 *Phys. Rev.* A **43** 5537–40
[6] Shibkov A A, Golovin Yu I, Zheltov M A, Korolev A A and Vlasov A A 2001 *Kristallografia* **46** 549–55 (Engl. transl. 2001 *Cryst. Rep.* **46** 496–501)
[7] Shochet O and Ben-Jacob E 1993 *Phys. Rev.* E **48** R4168–71
[8] Martiouchev L M and Seleznev V D 2000 *Dokl. Akad. Nauk* **371** 466–68 (Engl. transl. 2000 *Dokl. Phys.* **45** 129–31)
[9] Martiouchev L M, Kuznetsova I E and Seleznev V D 2000 *Zh. Eksp. Teor. Fiz.* **118** 149–62 (Engl. transl. 2000 *JETP* **91** 132–45)
[10] Ziegler H 1983 *An Introduction to Thermomechanics* (Amsterdam: North-Holland)
[11] Prigogine I 1955 *Introduction to Thermodynamics of Irreversible Processes* (Springfield, IL: US Department of Commerce)
[12] Nicolis G and Nicolis C 1980 *Q. J. R. Meteorol. Soc.* **106** 691–706
[13] Ben-Jacob E and Garik P 1990 *Nature* **343** 523–30
[14] Wang Mu and Ming Nai-ben 1993 *Phys. Rev. Lett.* **71** 113–6
[15] Hill A 1990 *Nature* **348** 426–8
[16] Sawada Y 1984 *J. Stat. Phys.* **34** 1039–45
[17] Martiouchev L M, Kuznetsova I E and Seleznev V D 2002 *Zh. Eksp. Teor. Fiz.* **121** 363–71 (Engl. transl. 2002 *JETP* **94** 307–14)
[18] Parker R 1970 Crystal growth mechanisms: energetics, kinetics and transport *Solid State Physics* vol 25 (New York: Academic)
[19] Kotler G R and Tiller W A 1967 *Proc. Int. Conf. on Crystal Growth (Boston, MA, 1966)* ed H S Peiser (Oxford: Pergamon)
[20] Mullins W W and Sekerka R F 1963 *J. Appl. Phys.* **34** 323–9
[21] Coriell S R and Parker R L 1965 *J. Appl. Phys.* **36** 632–7
[22] De Groot S R and Mazur P 1962 *Nonequilibrium Thermodynamics* (Amsterdam: North-Holland)
[23] Martiouchev L M and Sal'nikova E M 2002 *Pis. Zh. Tekh. Fiz.* **27** 80–8 (Engl. transl. 2002 *Tech. Phys. Lett.* **28** 242–5)